

## Biomimetic Surface Modifications Based on the Cyanobacterial Iron Chelator Anachelin

Stefan Zürcher,<sup>\*,†,§</sup> David Wäckerlin,<sup>†</sup> Yann Bethuel,<sup>‡</sup> Barbora Malisova,<sup>†</sup> Marcus Textor,<sup>†</sup> Samuele Tosatti,<sup>†,§</sup> and Karl Gademann<sup>\*,‡</sup>

Laboratory for Surface Science and Technology, Department of Materials, Surface SolutionS GmbH, and  
Laboratorium für Organische Chemie, Department of Chemistry and Applied Biosciences, ETH Zurich,  
Wolfgang-Pauli-Strasse 10, CH-8093 Zurich, Switzerland

Received September 12, 2005; E-mail: gademann@org.chem.ethz.ch, stefan.zuercher@mat.ethz.ch

The nonspecific adsorption of proteins, carbohydrates, cells, and other biological entities to surfaces (i.e., biofouling) constitutes a significant challenge in areas ranging from biomedical devices to marine technology.<sup>1</sup> Surface modification via poly(ethylene glycol) (PEG)-grafted polymers or self-assembled monolayers (SAM) offers the possibility of inhibiting biofouling.<sup>2</sup> In fact, to graft PEG onto surfaces, various strategies have been developed that rely on favorable thiol,<sup>2b</sup> silane,<sup>2d</sup> or polyelectrolyte<sup>2e</sup> interactions with metals, oxides, or polymeric substrates. Moreover, biomimetic coating strategies drawn from mussel adhesive protein (MAP) sequences mimicking mussel adhesion have been reported.<sup>3</sup>

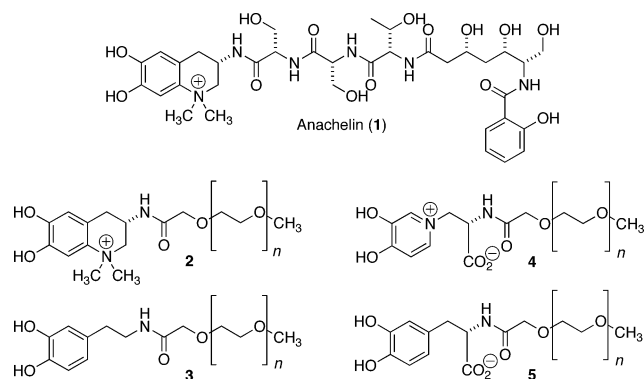
In this context, we note that many microorganisms are known to secrete small molecules (so-called *siderophores*), which have been evolutionarily optimized to efficiently bind to iron ions.<sup>4</sup> In addition, recent reports suggest that these siderophores recognize iron oxides<sup>5a</sup> and promote biofilm formation by cell adhesion to TiO<sub>2</sub> surfaces.<sup>5b</sup> We hypothesized that the strong binding forces of siderophores could be utilized to bind functional molecules to metal oxide surfaces. In this communication, we present a novel biomimetic strategy for surface modification that exploits the evolutionary optimized strong binding affinities of iron chelators such as anachelin (**1**)<sup>6</sup> (Chart 1). We demonstrate that a fragment of **1** conjugated to PEG (i.e., **2**) effectively binds to titanium oxide surfaces, thus allowing for the generation of stable, protein-resistant, nonfouling surfaces.

The target PEG–anachelin conjugate **2** is characterized by its catechol moiety, which is structurally similar to key elements of MAP sequences.<sup>3</sup> In addition, our approach employs a positive charge, which should allow for increased affinity of this compound to negatively charged surfaces. To probe these electrostatic effects, both control compounds **3** and **4** were prepared, which either lack a positive charge (such as **3**) or are zwitterionic (such as **4**). Finally, the DOPA conjugate **5** was prepared according to the literature.<sup>3c</sup> As substrate, we chose TiO<sub>2</sub> because this oxide was shown to participate in siderophore-mediated biofilm formation,<sup>5b</sup> and due to its importance related to applications in the fields of medical devices or optical biosensors.

First, suitable adsorption conditions for adlayer formation on TiO<sub>2</sub> needed to be identified. Layer thickness, which is proportional to the amount of PEG adsorbed,<sup>3c</sup> was then measured by use of variable angle spectroscopic ellipsometry (VASE) complemented by X-ray photoelectron spectroscopy (XPS) measurements.

PEG–anachelin conjugate **2** was thus adsorbed from a dilute aqueous solution under cloud point conditions<sup>7</sup> to maximize the PEG surface density, an essential aspect of nonfouling surface

**Chart 1.** Cyanobacterial Iron Chelator Anachelin (**1**), Its mPEG-5000 Conjugate Derivative **2** and Control Polymers **3–5**



properties.<sup>3c</sup> Cloud point conditions, which reduce the radius of gyration of the PEG-chains, can be achieved by a combination of increased temperature and ionic strength. After identifying optimal conditions (50 °C, 1.2 M ionic strength, K<sub>2</sub>SO<sub>4</sub>/NaCl 1:1), an adlayer thickness of about 3 nm for the iron chelator-derived compound **2** was measured after a short water rinse (Figure 1, top). In contrast to these excellent results, the adsorption of the control polymers **3–5** resulted in an overall lower thickness (and thus reduced PEG density) for **3** and **4** and no adlayer formation for **5**.

Furthermore, the binding strength of the anchoring group toward the substrate surface is of crucial importance for the stability of the adlayer. When reducing the temperature and ionic strength from the values used in the assembly process to those characteristic of “normal” (e.g., physiological) conditions, the PEG layer will swell, and the induced steric repulsive forces may exceed the adhesion strength of the assembled molecules, resulting in the partial loss of molecules and reduced PEG surface density<sup>3c</sup> and, consequently, lower protein resistance.<sup>2e</sup> To investigate this aspect, the coated samples were incubated at physiological conditions for 48 h, and the adlayer thickness was examined. In the cases of **2** and **3**, we observed (by VASE) an adlayer thickness reduction of roughly 40% to 1.7 and 1.2 nm, respectively. For the zwitterionic compound **4**, a complete loss of adsorbate was observed. This notion is supported by XPS measurements indicating the presence of the PEG characteristic C–O component both in the C 1s and O 1s signal of the spectra in the cases of **2** and **3**, but not of **4** and **5** (data in Supporting Information).

Next, the protein resistance was evaluated upon exposure to full human serum. Notably, a reduction of the protein adlayer thickness of over 95% is observed by VASE for **2** and **3** in comparison to the bare TiO<sub>2</sub> surface (Figure 1, bottom). In contrast, the use of control polymers **4** and **5** resulted in a high protein adsorbed mass

<sup>†</sup> Laboratory for Surface Science and Technology.

<sup>‡</sup> Laboratorium für Organische Chemie der ETH Zürich.

<sup>§</sup> Surface SolutionS GmbH.

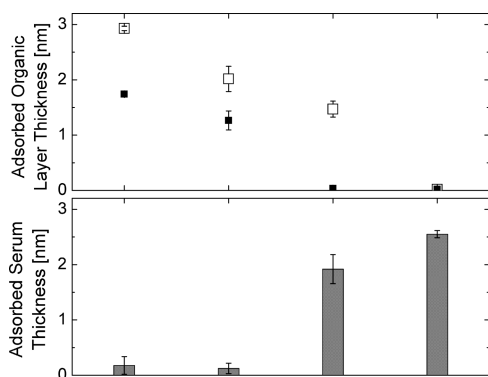


**Figure 1.** (Top) Layer thickness of compounds **2–5** directly after adsorption (open squares) and after immersion in physiological buffer solution for 2 d (black squares). (Bottom) Protein resistance measured via increase of layer thickness after immersion in full human serum.

that correlates with the lower adlayer thickness and correspondingly reduced PEG chain surface densities observed for those two polymers.

The structural reason for the remarkable differences observed for the four different headgroups resides in their overall charge pattern. In the first step, i.e. adsorption under high-salt conditions, the charge and electrostatic interactions with the surface are likely to contribute little to the overall adsorption kinetics in view of the correspondingly small Debye length (ca. 0.3 nm). However, in the second step, upon returning to lower ionic strength, the positive charge in the anachelin-derived compound **2** might favorably interact with the remaining negative hydroxylates on the oxide surface, thus increasing the overall binding stability. While such electrostatic effects are absent for neutral **3**, the negative carboxylates **4** and **5** are expected to be subject to repulsive electrostatic effects, which may contribute to the observed loss of molecules from the negatively charged TiO<sub>2</sub> surface during washing.

The stability of polymers **2** and **3** against aerobic oxidation was then evaluated. Dopamine itself is known to be prone to oxidation forming melanine-type dark and insoluble polymers.<sup>8</sup> In fact, oxidation of **3** (Figure 2a, red line, solid) was readily observed after 1 d exposure to air at room temperature by UV/vis spectroscopy (Figure 2a, red line dashed). The appearance of a band at 350 nm results from the oxidation of dopamine-derived **3**. The decomposition is also directly visible, as the solution of **3** turns brown over time (Figure 2b). In strong contrast, the anachelin-derived **2** resisted oxidation (Figure 2a, black lines), as has been also shown for the anachelin chromophore.<sup>9</sup>

In conclusion, we have developed a novel biomimetic strategy based on the iron chelator anachelin for the formation of a stable, protein-resistant adlayer. The natural product-derived PEG conjugate **2** displayed superior properties in terms of adlayer thickness, protein resistance as well as binding strength, and in particular oxidative stability when compared to control polymers **3–5**. We speculate that the positive charge combined with the remarkable surface properties of catechols such as in **2** positively influence the adlayer formation and stability and thus complement MAP-based approaches.<sup>3b–e</sup> Current efforts are directed toward the application

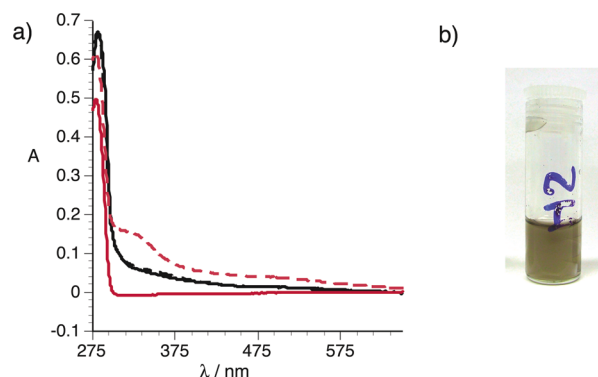


**Figure 2.** (a) UV/Vis spectra showing the degree of oxidation of **2** (black line) and **3** (red line) after 0 h (solid lines) and 24 h (dashed lines); (b) solution of **3** (HEPES 2 buffer, 1 mg/ml) after 10 d of storage showing decomposition.

of siderophore SAMs to other types of surfaces/substrates and for related technological applications.

**Acknowledgment.** K.G. thanks Prof. Dr. Erick M. Carreira for financial support in the context of his habilitation. Financial support from the SNF (Ph.D. fellowship to Y.B.) is gratefully acknowledged.

**Supporting Information Available:** Synthetic protocols of the four PEGylated polymers and XPS data. This material is available free of charge via the Internet at <http://pubs.acs.org>.

## References

- Reviews: Costerton, J. W.; Lewandowski, Z.; Caldwell, D. E.; Korber, D. R.; Lappin-Scott, H. M. *Annu. Rev. Microbiol.* **1995**, *49*, 711–745; Hall-Stoodley, L.; Costerton, J. W.; Stoodley, P. *Nature Rev. Microbiol.* **2004**, *2*, 95–108.
- (a) Lee, J. H.; Kopecek, J.; Andrade, J. D. *J. Biomed. Mater. Res.* **1989**, *23*, 351–368. (b) Prime, K. L.; Whitesides, G. M. *Science* **1991**, *252*, 1164–1167. (c) Desai, N. P.; Hubbell, J. A. *Biomaterials* **1991**, *12*, 144–153. (d) Yang, Z.; Galloway, J. A.; Yu, H. *Langmuir* **1999**, *15*, 8405–8411. (e) Pasche, S.; De Paul, S. M.; Vörös, J.; Spencer, N. D.; Textor, M. *Langmuir* **2003**, *19*, 9216–9225.
- (a) Waite, J. H.; Tanzer, M. L. *Science* **1981**, *212*, 1038–1040. (b) Dalsin, J. L.; Hu, B.-H.; Lee, B. P.; Messersmith, P. B. *J. Am. Chem. Soc.* **2003**, *125*, 4253–4258. (c) Dalsin, J. L.; Lin, L.; Messersmith, P. B.; Tosatti, S.; Vörös, J.; Textor, M. *Langmuir* **2005**, *21*, 640–646. (d) Statz, A. R.; Messersmith, P. B.; Meagher, R. J.; Barron, A. E. *J. Am. Chem. Soc.* **2005**, *127*, 7972–7973. (e) Sever, M. J.; Weissner, J. T.; Monahan, J.; Srinivasan, S.; Wilker, J. J. *Angew. Chem., Int. Ed.* **2004**, *43*, 448–450. (f) Xu, C.; Xu, K.; Gu, H.; Guo, Z.; Xu, B.; Zheng, R.; Liu, H.; Zhang, X. *J. Am. Chem. Soc.* **2004**, *126*, 9938–9939. (g) Rundqvist, J.; Haviland, D. B.; Hoh, J. H. *Langmuir* **2005**, *21*, 2981–2987. (h) Fan, X.; Lin, L.; Dalsin, J. L.; Messersmith, P. B. *J. Am. Chem. Soc.* **2005**, *127*, 15843–15847.
- Review: Raymond, K. N.; Dertz, E. A.; Kim, S. S. *Proc. Natl. Acad. Sci. U.S.A.* **2003**, *100*, 3584–3588 and references therein.
- (a) Reviews: Stone, A. T. *Rev. Mineral.* **1997**, *35*, 309–344; Kraemer, S. M. *Aquat. Sci.* **2004**, *66*, 3–18 and references therein. (b) McWhirter, M. J.; Bremer, P. J.; Lamont, I. L.; McQuillan, A. *J. Langmuir* **2003**, *19*, 3575–3577.
- Isolation: Beiderbeck, H.; Taraz, K.; Budzikiewicz, H.; Walsby, A. E. *Z. Naturforsch., C: Biosci.* **2000**, *55*, 681–687; Itou, Y.; Okada, S.; Murakami, M. *Tetrahedron* **2001**, *57*, 9093–9099. Synthesis: Gademann, K.; Bethuel, Y. *Angew. Chem., Int. Ed.* **2004**, *43*, 3327–3329. Gademann, K.; Bethuel, Y. *Org. Lett.* **2004**, *6*, 4707–4710.
- Kingshott, P.; Thissen, H.; Griesser, H. J. *Biomaterials* **2002**, *23*, 2043–2056.
- Review: Mason, H. S. *Annu. Rev. Biochem.* **1965**, *34*, 595–634.
- Bethuel, Y.; Gademann, K. *J. Org. Chem.* **2005**, *70*, 6258–6264.

JA056256S